OPEN ACCESS
Journal of Multidisciplinary Applied Natural Science Vol. 6 No. 3 (2026) https://doi.org/10.47352/jmans.2774-3047.463
Check for updates
Research Article

Soliton Area Theorem for the Cubic Complex Ginzburg-Landau Equation with Drift and Defect in an Electromagnetic Dissipative System

Nonis Airina Mohd Arshad, Ahmad Fateh Mohamad Nor, Nazirah Ramli, and Nur Izzati Khairudin*

Received : December 1, 2025	Revised : February 20, 2026	Accepted : June 2, 2026	Online : July 27, 2026

Abstract
This paper presents an approximate ansatz-based solution of the cubic complex Ginzburg-Landau equation (CCGLE) influenced by electromagnetic drift and defect. This study is carried out within the area theorem framework, which describes a relation between soliton energy and duration in dissipative systems. Within this framework, a hyperbolic cosine ansatz is applied to obtain approximate expressions for the soliton energy and duration in the non-integrable dissipative system. From the derivation, the real parameter B in the ansatz is identified as a shape-controlling parameter, which results in three cases known as case I for $|B|<1$, case II for $B > 1$, and case III for $B = 0$. Based on these cases, front stationary solitons are obtained through the balance between the two-parameter family involving non-linearity and dispersion, as well as gain and loss, together with the interaction between drift and defect mechanisms. These interactions allow the system to self-organize into a stable localized structures within the dissipative system. Variations in the parameter B slightly change the soliton profile, especially in terms of width and amplitude. Furthermore, the drift parameter c is varied at $c \in \{-0.10, 0.60, 0.95\}$ to investigate the behavior of the area theorem in the CCGLE, where the soliton solutions remain localized during propagation. Overall, the results indicate that the proposed approximate ansatz-based solution is able to describe localized dissipative structures in the non-integrable CCGLE with drift and defect effects.

Keywords: area theorem, dissipative solitons, Ginzburg-Landau equation, stationary solitons

1. INTRODUCTION

Dissipative solitons are localized waves that can travel across a medium while maintaining their shape in the presence of energy gain and loss [1]. The stability of dissipative solitons is achieved through a two-parameter family balance, which includes the balance of non-linearity and dispersion, as well as gain and loss [2][3]. The notion of dissipative solitons based on three fundamental concepts: classical soliton theory, nonlinear dynamics, and Prigogine's theory of self-organization. The idea of solitons first began in conservative and integrable systems, where stable waves are formed when dispersion, which tends to spread the wave, is balanced by nonlinearity that helps maintain its shape [3]. However, many real physical systems are dissipative because energy continuously shifts with the surroundings. This causes the creation of dissipative solitons in non-integrable systems such as the Complex Ginzburg-Landau Equation (CGLE), where soliton stability becomes more complex due to the additional balance between gain and loss [3]-[6]. Since the CGLE is a non-integrable system, obtaining exact analytical solutions is difficult, and therefore approximation and numerical methods are commonly used to study dissipative soliton behaviour. According to non-linear dynamics, dissipative solitons are stable fixed points in a infinite-dimensional system where small variations in system parameters can cause bifurcations and transform the soliton into different behavior such as pulsating, erupting, snaking, creeping, or chaotic solitons [5][6]. Furthermore, Prigogine's theory states that dissipative solitons are self-organized structures that emerge in nonequilibrium systems by continuous energy exchange with their surroundings [4]-[6]. Therefore, these three notions are important in explaining the formation, stability, and evolution of dissipative solitons in complex nonlinear dissipative systems.

One of the most well-known nonlinear mathematical models in dissipative solitons is the CGLE [7]. The CGLE is known as an amplitude-modulation equation where a nonlinear partial differential equation (PDE) models a system that

Table 1. Fixed parameters used for the obtained soliton profiles [2][14].

Parameter	Value
D	1.00
δ	-0.10
β	0.08
γ	1.00
ε	-0.66
c	0.12
h	0.075

has a finite number of degrees of freedom [3][6]. It can shed light on the stability and dynamics of the solitons and show how they behave under different conditions [8]. This study focuses on the cubic CGLE (CCGLE) [5] with the additional drift and defect mechanisms, which can be written as Equation (1);

$$\partial_z A = \delta A + \left(\beta + i\frac{D}{2}\right)\partial_x^2 A + (\varepsilon + i\gamma)|A|^2 A - c\partial_z A + b(x), \tag{1}$$

where $A = A(x,z)$ is a complex function of the retarded time x and propagation distance z. Here, D is the group velocity dispersion (GVD), γ is the cubic nonlinearity, δ is the linear loss, ε is the nonlinear gain, and β is the spectral filtering coefficient. The drift is represented by the coefficient c, while the defect term $b(x)$ is defined by a single Gaussian profile $b(x) = h\exp\left[-\left(\frac{x-x_0}{\sigma}\right)^2\right]$, where h is the height, σ is the half-width, and x_0 is the centre of the defect, respectively.

Despite the CGLE being a highly complex model, it is not always sufficient to capture what really happens in systems [5][6]. Sometimes, real-world systems are more complex and often involve other effects [9]. This has led researchers to extend the equation in various ways. For instance, some studies capture more complex soliton behaviors by adding Kerr and cubic-quintic non-linearities, higher-order dispersion, and saturable gain [9]-[12]. Each extension has its own capabilities and functions within the system.

The drift and defect are two additional mechanisms that could be added into the CCGLE to extend its dynamical behavior. The drift term describes how external forces influence soliton motion, leading to oscillatory behavior and changes in stability [13]. On the other hand, defects are spatial inhomogeneities that have the ability to pin or localize the soliton and act as sources of perturbations that make the soliton excitable [13][14]. In optical systems, these effects are usually seen as external disturbances that affect pulse motion and small imperfections in the medium [15]-[18]. The interaction between drift and defect has been shown to produce rich dynamical behaviors in dissipative systems, such as the Swift-Hohenberg Equation (SHE) [13]-[17]. The drift introduces a velocity offset that breaks spatial symmetry, allowing the soliton to move or remain stable [15][16], while the defect tends to stabilize or pin the soliton depending on system parameters [17]. The interplay of drift and defect can result in stable, stationary, or controlled oscillatory states [14]-[17]. Despite these insights, the combined effect of drift and defect in the CCGLE has not been systematically analyzed. This motivates this study to investigate how these mechanisms influence the dynamics and characteristics of dissipative solitons.

Two assumptions are made in this study. First, drift and defect are included in the system as additional mechanisms to investigate their influence on dissipative soliton dynamics. Second, the CCGLE is chosen instead of the cubic-quintic CGLE for analytical simplicity [19]. The CCGLE can reduce the number of free parameters while still providing valuable insights into soliton behavior. The inclusion of drift and defect already increases system complexity [15][16], making this choice practical for the present study [8]. Furthermore, this study seeks to construct an approximate ansatz-based solution of Equation (1) using the formulation from Renninger [20]. The solution is obtained by applying a hyperbolic-cosine ansatz to Equation (1), where the real parameter B acts as a shape-controlling factor that determines the soliton profile. Depending on the value of B, three different solution cases are identified: case I, $|B| < 1$; case II, $B > 1$; and case III, $B = 0$. These cases allow the exploration of different soliton shapes and behaviors under the influence of drift and defect.

One of the main analytical tools for describing solitons is the soliton area theorem, which shows a relationship between soliton energy and soliton duration for localized solutions of the CGLE [20]. In previous work, Renninger [20] derived the soliton area theorem for the cubic-quintic CGLE without additional terms to interpret numerical and experimental results. Since then, this theorem has been widely referenced in studies of dissipative solitons [20][23]. Although the original area theorem was derived for the cubic-quintic CGLE [20], the main idea of relating soliton energy and duration for localized dissipative solutions is still applicable to the CCGLE. In this study, the area theorem is used as an analytical framework to examine the effects of drift and defect on this relationship.

Recent studies have investigated analytical solutions of the complex Ginzburg-Landau equation with various types of non-linearities [21]. Specifically, Kudryashov [21] studied a polynomial nonlinearity of four powers and obtained exact traveling wave solutions expressed via elliptic functions without constraints on the parameters. In addition, Wang [22] studied the pure-cubic CGLE with Kerr and power-law nonlinearities, constructing traveling wave solutions through the complete discrimination system for polynomials and analyzing soliton stability and chaotic behaviors. Collectively, these studies highlight ongoing interest in deriving analytical solutions and understanding soliton dynamics under different nonlinearities, motivating the approach adopted in the present work.

The focus of this study is to analyze the behavior of the soliton area theorem in the CCGLE with drift and defect mechanisms. The drift parameter c is varied while the defect is kept fixed in order to observe its effect on localized dissipative structures. Within the approximate ansatz-based solution, the shape parameter B determines different solution regimes corresponding to distinct localized behaviors. The competition between drift and defect governs whether the system supports stationary localized structures or other types of behavior.

2. SOLITON AREA THEOREM

This section presents an approximate ansatz-based solution of Equation (1) using a hyperbolic-cosine ansatz. The ansatz describes the localized wave structure and simplifies the governing equation into algebraic relations for the soliton parameters. Based on these relations, expressions for the soliton energy are derived. The soliton duration is then determined using the full width at

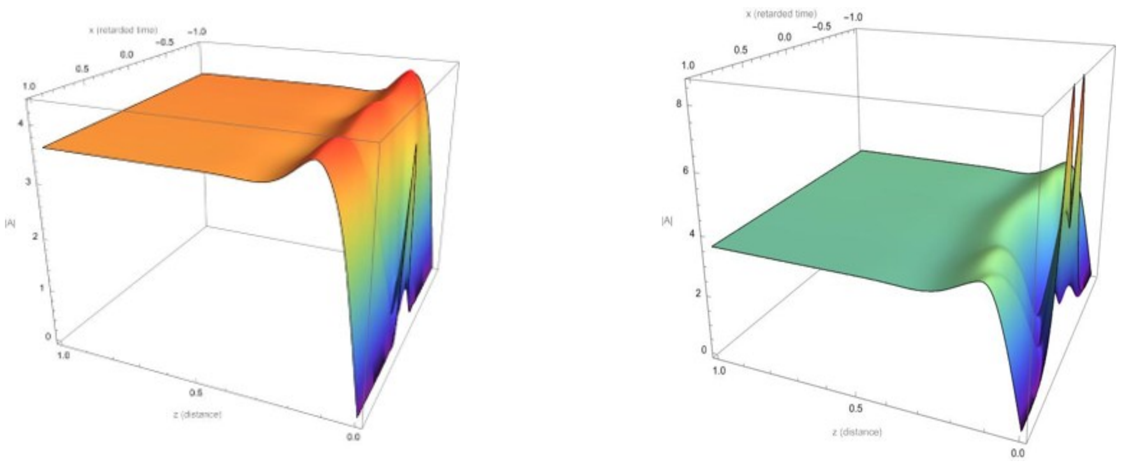

(a) **(b)**

Figure 1. Front stationary soliton profiles of the CCGLE with drift and defect for case I with a parameter variation of $|B| < 1$. (a) $B = 0.217$ and (b) $B = 0.5$.

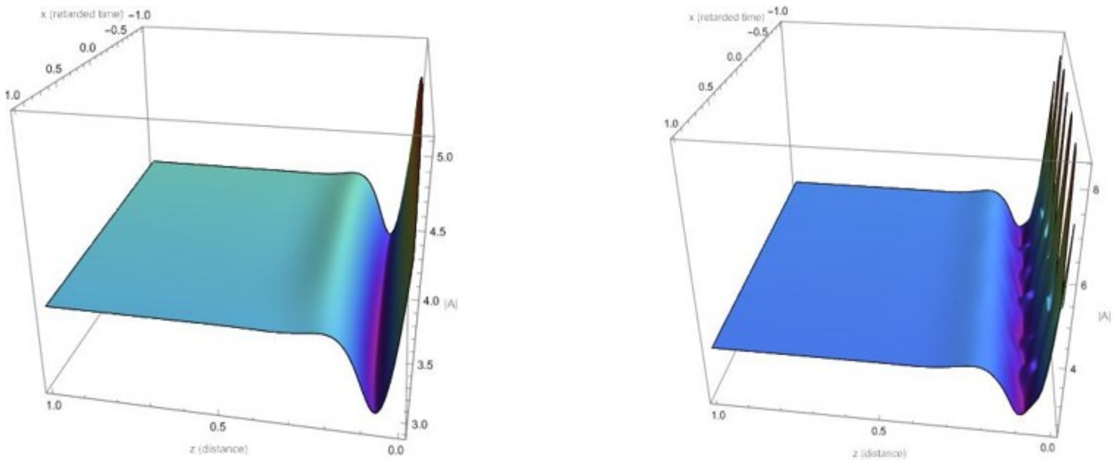

(a) **(b)**

Figure 2. Front stationary soliton profiles of the CCGLE with drift and defect for case II with a parameter variation of $B > 1$. (a) $B = 1.5$, and (b) $B = 2.217$.

half maximum (FWHM) of the intensity profile.

2.1. Definition of the Ansatz and Derivation of Relations

The hyperbolic cosine ansatz is used to describe the soliton profile. The ansatz is written as Equation (2) [20];

$$A(x,z)=\sqrt{\frac{M}{\cosh\left(\frac{x}{\tau}\right)+B}}\,e^{-i\frac{\rho}{2}\ln\left(\cosh\left(\frac{x}{\tau}\right)+B\right)+i\eta z} \quad \textbf{(2)}$$

where M, B, τ, ρ and η are real constants representing the soliton amplitude, shape parameter, width, chirp, and phase shift, respectively. In this framework, the shape parameter B controls the profile of the localized structure and determines its degree of localization. The relations are obtained using a center-matched approximation, where the ansatz is applied at the pulse center $x = 0$. This reduces the governing partial differential equation into a set of algebraic consistency conditions. This approach gives an approximate description of stationary localized solutions rather than an exact solution of the full system, but it is sufficient to study the energy and duration of the soliton.

By substituting Equation (2) into Equation (1), the complex equation is simplified into algebraic forms. Separating the real and imaginary parts yields two governing equations. The real part corresponds to the amplitude and gain-loss balance, expressed as Equation (3).

$$\delta+\frac{\rho D-2\beta}{4\tau^2(1+B)}+\frac{\varepsilon M}{1+B}+\frac{h\cos(\phi)\sqrt{1+B}}{\sqrt{M}}=0 \quad \textbf{(3)}$$

This relation represents the balance between conservative effect, dissipative terms, and the effect of the defect, which determines the condition for a stationary solution. The fourth term of Equation (3) indicates that the defect strength is coupled with the amplitude M and phase ϕ parameters to support a stationary state. This suggests that the defect contributes to the gain and loss balance required for a self-sustained soliton within the approximate ansatz-based solution.

The imaginary parts govern the phase and frequency shift, presented as Equation (4);

$$\frac{\gamma M}{1+B}-\frac{(2\rho\beta+D)}{4\tau^2(1+B)}-\frac{h\sin(\phi)\sqrt{1+B}}{\sqrt{M}}=(1+c)\eta \quad \textbf{(4)}$$

where $\phi=-\frac{\rho}{2}\ln(1+B)+\eta z$, related to the frequency shift η of the soliton. The drift coefficient c appears directly in the term $(1 + c)\eta$. This suggests that the presence of drift changes the required value of η to remain stationary. The other terms describe the balance between nonlinearity, dispersion, and the phase effect of the defect. Thus, Equations (3) and (4) indicate the relationship between the soliton parameters (M, τ, ρ, B, η) and system parameters (δ, β, D, ε, γ, c, h). The detailed derivation steps are provided in Appendix A.

From Equation (3), the amplitude M can be obtained explicitly by applying Cardano's formula and is given by Equation (5);

$$M = \left[-\frac{q}{2} \pm \sqrt{\left(\frac{q}{2}\right)^2 + \left(\frac{p}{3}\right)^3} \right]^{\frac{2}{3}} \tag{5}$$

where $p = \frac{1}{\varepsilon}\left(\delta(1+B) + \frac{\rho D - 2\beta}{4\tau^2} \right)$ and $q = \frac{h\cos(\phi)(1+B)^{\frac{3}{2}}}{\varepsilon}$. The expression shows that the amplitude is determined by the balance between gain and loss, dispersion, nonlinearity, and the defect strength. The soliton scale τ and phase constant η are determined from Equation (4) as follows Equation (6),

$$\tau = \sqrt{\frac{2\rho\beta + D}{4[\gamma M - (1+B)(1+c)\eta - \frac{h\sin(\phi)(1+B)^{\frac{3}{2}}}{\sqrt{M}}}} \tag{6}$$

and

$$\eta = \left(\frac{1}{1+c}\right)\left(\frac{\gamma M}{1+B} - \frac{(2\rho\beta + D)}{4\tau^2(1+B)} - \frac{h\sin(\phi)\sqrt{1+B}}{\sqrt{M}} \right). \tag{7}$$

From Equation (6), the soliton width τ depends on dispersion, nonlinearity, drift, and defect. This suggests that drift may indirectly affect the soliton width. Equation (7) describes the propagation behavior of the soliton, which is also affected by system parameters including drift and defect.

Therefore, Equations (3) - (7) provide an approximate set of consistency relations describing stationary localized solutions in the CCGLE with drift and defect. These relations describe how the amplitude, width, and soliton phase depend on the system parameters. This framework provides the basis for the area theorem formulation in the following sections.

2.2. Derivation of Soliton Energy, E(B), and the Shape-dependent Function F(B) for Each Regime of B

The soliton energy, E, is defined as the integral of the soliton intensity over the retarded time,

$$E = \int_{-\infty}^{\infty} \left| A(x,z) \right|^2 dx \tag{8}$$

By substituting the hyperbolic cosine ansatz from Equation (2) into Equation (8), the soliton energy can be expressed in the compact form as follows Equation (9);

$$E(B) = MF(B) \tag{9}$$

where M and τ denote the soliton amplitude and width, respectively. The explicit form of *F(B)* depends on the value of the shape parameter B, leading to three different mathematical regimes:

Case I: $|B| < 1$

$$F(B) = \frac{2\tau\cos^{-1}(B)}{\sqrt{1-B^2}} \tag{10}$$

In this regime (Equation (10)), the shape parameter satisfies $|B| < 1$, leading to a bounded inverse cosine function. The corresponding soliton profile is smooth and localized, with a finite width.

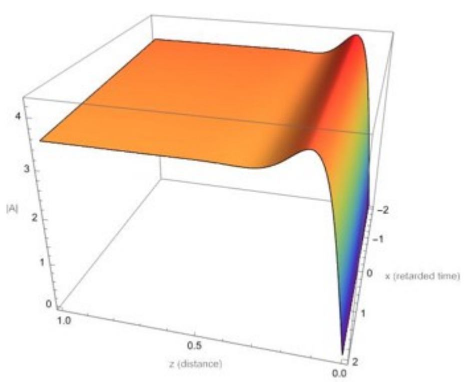

Figure 3. Front stationary soliton profiles of the CCGLE with drift and defect for case III, $B = 0$.

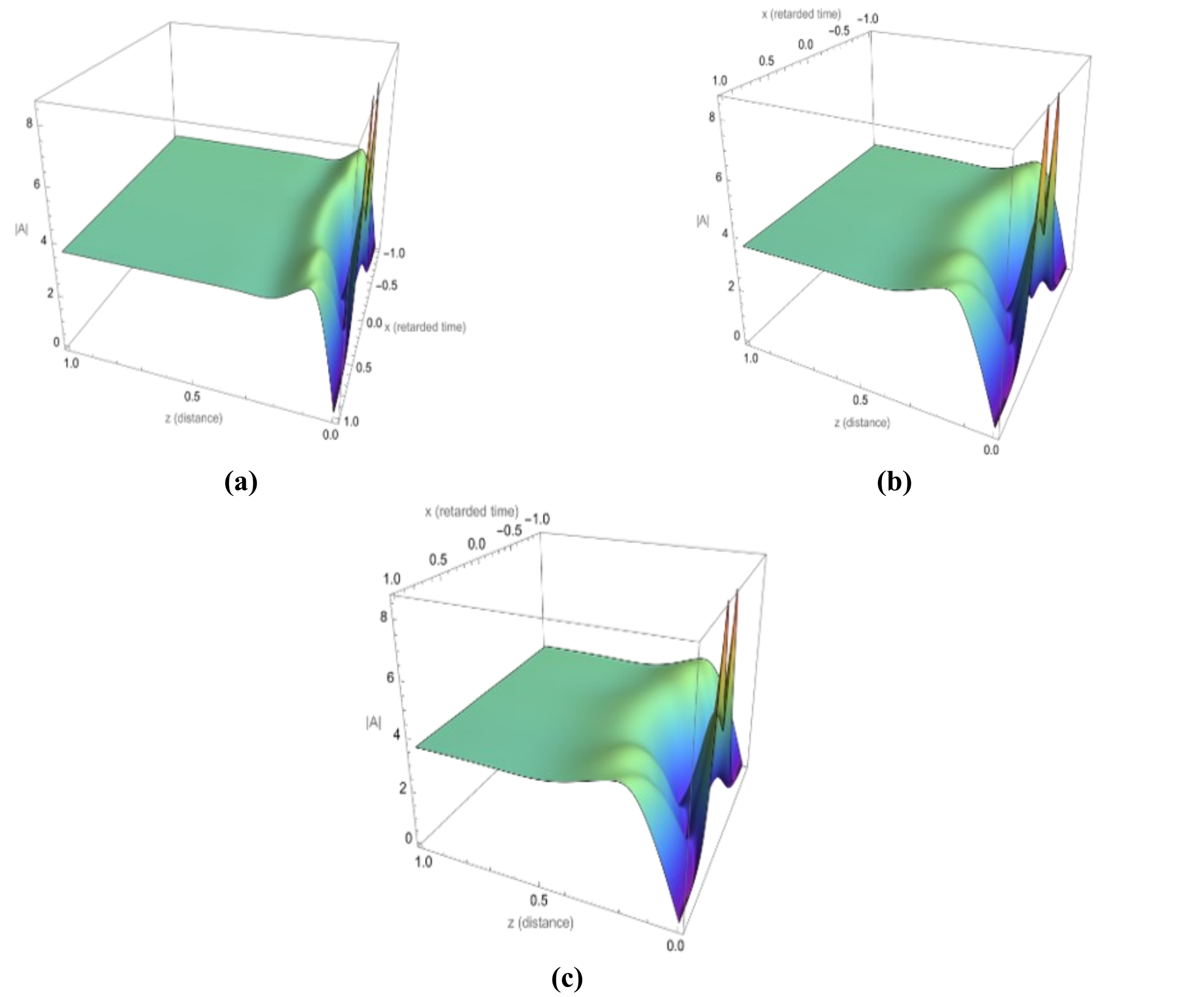

Figure 4. Front stationary soliton profiles for case I, $B = 0.5$ under variation of drift parameter c: (a) $c = -0.10$, (b) $c = 0.60$, and (c) $c = 0.95$.

The energy varies continuously with B, indicating a stable bell-shaped soliton solution.

Case II: $B > 1$

$$F(B) = \frac{2\tau \cosh^{-1}(B)}{\sqrt{B^2 - 1}} \quad \textbf{(11)}$$

When $B > 1$, the inverse hyperbolic cosine function governs the soliton shape. This regime (Equation (11)) corresponds to strongly localized dissipative solitons with enhanced soliton width. The nonlinear dependence of *F(B)* on *B* reflects the influence of drift and defect parameters on the soliton energy.

Case III: $B = 0$

$$F(B) = \pi\tau \quad \textbf{(11)}$$

For the special case $B = 0$, the soliton energy reduces to a constant value proportional to the soliton width (Equation (12)). This case remains as a well-defined localized pulse with finite amplitude and width, but with the simplest symmetric profile. The detailed integration procedure is presented in Appendix B for completeness. This result reveals that the soliton energy is directly controlled by the soliton amplitude, width, and the shape parameter B, highlighting the influence of drift and defect through the soliton parameters. Physically, the energy increases with amplitude and width and varies nonlinearly with the shape parameter B.

2.3. Derivation of Soliton Duration, T(B) and the Final Area-Theorem Relation between E(B) and T (B)

The soliton duration is evaluated using the FWHM of the soliton amplitude profile. The

FWHM, denoted as T, is defined as the temporal width between the two points $x = \pm x_0$, where the intensity drops to half of its peak value. This is expressed by the condition of Equation (13).

$$\left|A(x_0)\right|^2 = \frac{1}{2} \cdot \left|A(0)\right|^2 . \qquad \textbf{(13)}$$

Substituting the intensity profile into the FWHM condition given in Equation (13) leads to an equation involving the hyperbolic cosine function. By solving this equation, the half-maximum points are obtained. Due to the symmetry of the soliton profile about the pulse centre, the full width at half maximum is twice this value. Therefore, the FWHM soliton duration is given by Equation (14).

$$T(B) = 2\tau \cosh^{-1}(2 + B) \qquad \textbf{(14)}$$

This expression shows that the soliton duration depends on the soliton width parameter τ and the shape parameter B. Together with the soliton energy expression derived in Section 2.2, this result establishes a relationship between the soliton energy *E(B)* and soliton duration *T(B)*. Thus, the soliton area theorem provides a relation between the soliton energy *E(B)* and duration *T(B)*. The expression of the soliton energy is presented as Equation (15),

$$E(B) = MF(B) \qquad \textbf{(15)}$$

where the shape function *F(B)* is given in the following piecewise function Equation (16),

$$F(B) = \begin{cases} \dfrac{2\tau \cos^{-1}(B)}{\sqrt{1-B^2}} & , |B| < 1 \\ \dfrac{2\tau \cosh^{-1}(B)}{\sqrt{B^2-1}} & , B > 1 \\ \pi\tau & , B = 0 \end{cases} . \qquad \textbf{(16)}$$

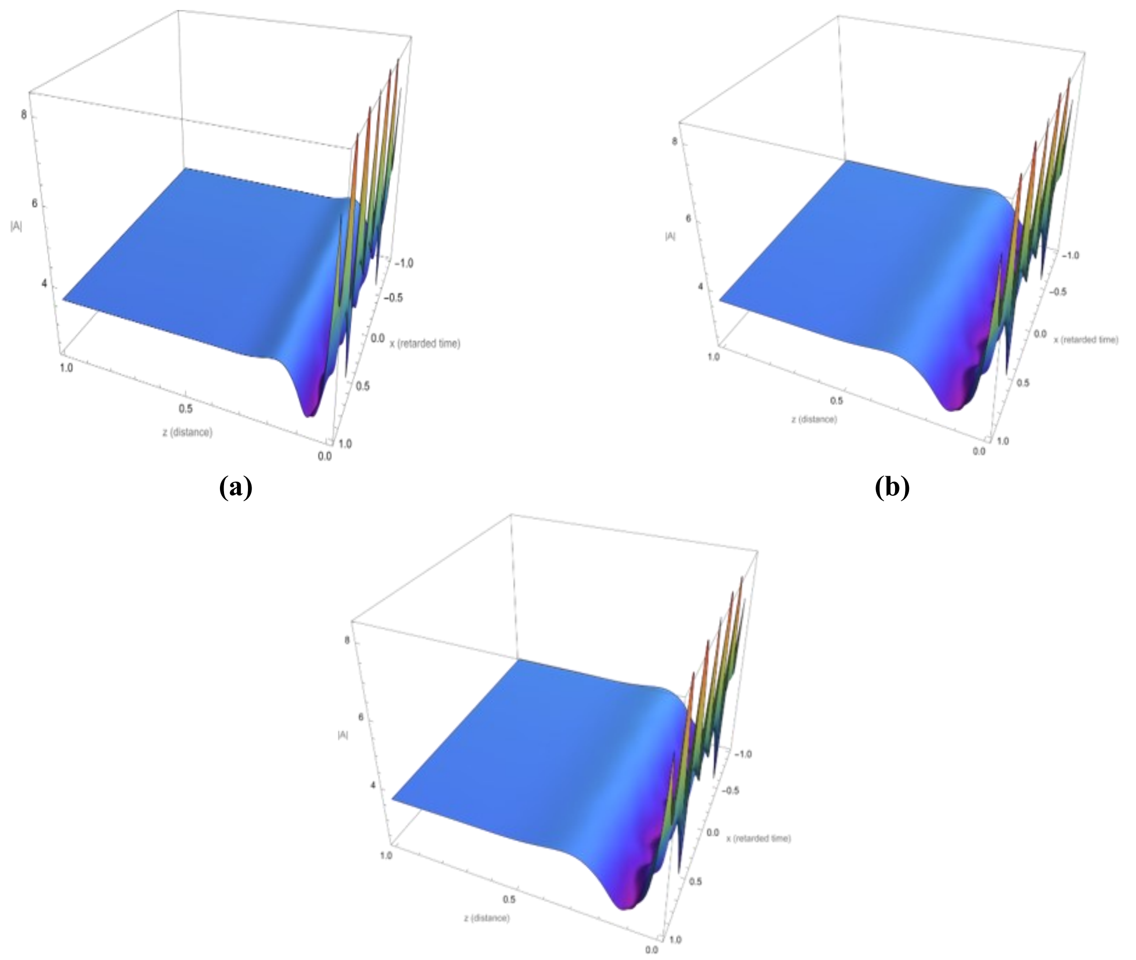

(a) **(b)** **(c)**

Figure 5. Front stationary soliton profiles for case II, $B = 1.5$ under variation of drift parameter c: (a) $c = -0.10$, (b) $c = 0.60$, and (c) $c = 0.95$.

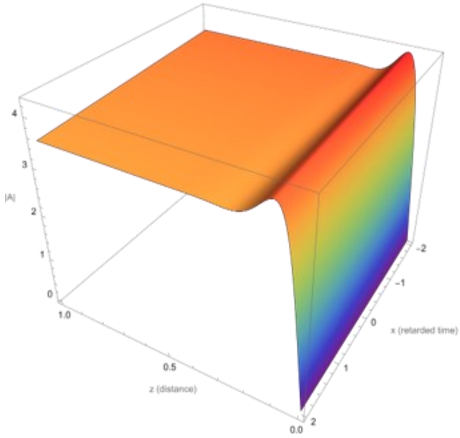

(a)

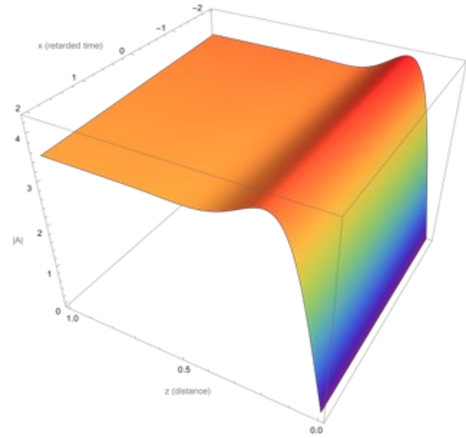

(b)

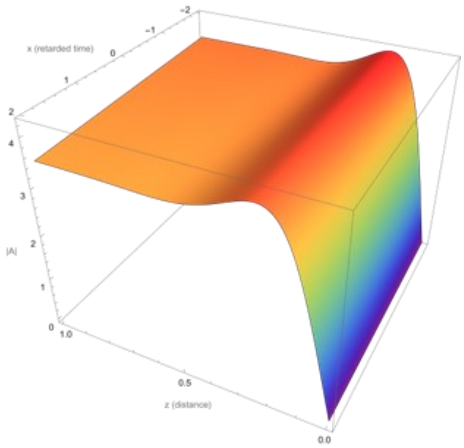

(c)

Figure 6. Front stationary soliton profiles for case III, $B = 0$ under variation of drift parameter c: (a) $c = -0.10$, (b) $c = 0.60$, and (c) $c = 0.95$.

and the FWHM soliton duration, $T(B)$, can be written as Equation (17).

$$T(B) = 2\tau \cosh^{-1}(2 + B). \tag{17}$$

These results show that both energy and duration depend on the shape parameter B, and indirectly reflect the influence of drift and defect through the soliton parameters derived from the ansatz-based solution, which is formulated within an approximate center-matched framework.

3. RESULTS AND DISCUSSIONS

This section discusses the behavior of the obtained front stationary soliton for different values of the parameter B, along with variations of the drift parameter c. The parameter values used throughout this section are summarized in Table 1, except for the drift parameter c, which is varied in Section 3.2.

Although the derivation in Section 2 is simplified at the pulse center by taking $x = 0$ and $x_0 = 0$, the graphical representation of the ansatz-based solution is performed over a finite domain of $L = 70$. The defect is centered at $x_0 = \frac{L}{2}$, so that the front stationary soliton structure can be clearly observed within the domain.

3.1. Graphical Representation of Soliton Profiles for Varying Parameter B

Figures 1 - 3 show the behavior of the front stationary soliton profiles for different values of the shape parameter B. Figure 1 corresponds to case I, $|B| < 1$, Figure 2 correspond to case II, $B > 1$, and Figure 3 corresponds case III, $B = 0$. In all cases, the solution maintains a front stationary soliton profile. However, changes in the parameter B produce variations in the amplitude and width of the soliton. For $|B| < 1$, the soliton becomes slightly wider with lower peak amplitude, while when $B > 1$, the soliton becomes sharper with higher peak intensity. When $B = 0$, the soliton shows a more flattened localized structure while still maintaining a front stationary soliton profile.

Despite the initial expectation that drift and defect may lead to more complex behaviors, Figures 1 – 3 show that the obtained stationary solitons maintain a front stationary soliton profile. Only minor changes in width and peak intensity are observed when the parameter B is varied. This indicates that, under the chosen parameter set, the system produces front stationary solitons profiles, even in the presence of drift and defect effects. The results show that Equation (16) describes a behavior of the localized structure across the considered cases.

The behavior observed here is align with recent studies on coupled cubic-quintic CGLE [25], which report that localized structures can maintain their shape under small parameter variations. Although the present system is cubic and includes inhomogeneities, the qualitative behavior is comparable in the sense that the localized profile remains preserved under parameter changes. This comparison suggests that the ansatz-based formulation in Equation (16) provides a useful approximation for describing front stationary soliton profiles in dissipative nonlinear systems.

3.2. Graphical Representation of Soliton Profiles for Varying Drift Parameter c

To examine the influence of drift on soliton behavior, the drift parameter c is varied while all other parameters are kept fixed, except c, as listed in Table 1. The drift parameter c is varied at $c \in \{-0.10, 0.60, 0.95\}$ for the three cases discussed in the previous section, as illustrated in Figures 4 – 6.

Figures 4 – 6 show the behavior of the obtained front stationary soliton profiles for each selected value of parameter B under different drift values. In all three cases, the amplitude and width of the soliton profile remain almost unchanged, while a slight shift in position is observed with increasing drift parameter c. This indicates that the drift parameter c mainly affects the spatial position of the front stationary soliton profile, without significantly altering its shape within the considered parameter range.

3.3. Verification with Previous Studies

Based on the results in Figures 1 – 6, the obtained solutions show a clear change in amplitude across the spatial domain. The soliton profile consists of two nearly constant regions which are separated by a sharp transition layer. This type of behavior is align with the front-type structures discussed by van Saarloos and Hohenberg [24]. Although the hyperbolic-cosine ansatz in Equation (2) is commonly used to describe localized pulse structure [20], the inclusion of electromagnetic drift and defect modifies the obtained profile into front-like stationary structure within the simulated domain.

As the drift parameter varies, the position and steepness of the transition layer change slightly, while the overall profile shape remains the same across the considered cases. Figure 7 illustrates a typical front structure in the one-dimensional CGLE

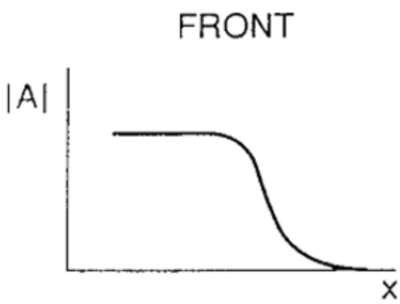

Figure 7. Typical front structure in the one-dimensional CGLE reproduced from van Saarloos and Hohenberg [24].

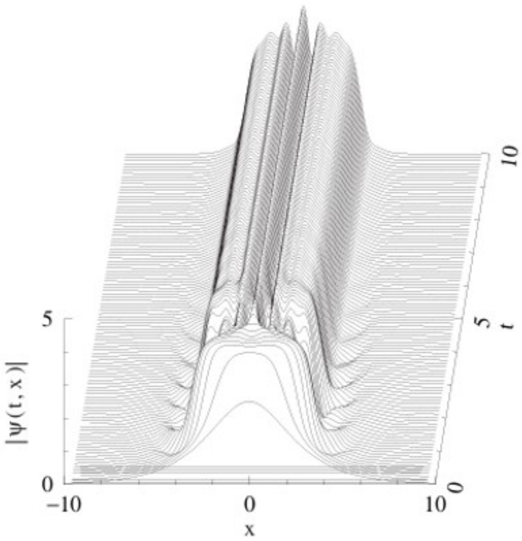

Figure 8. The class of stationary soliton solutions of the CSHE. Parameters of the simulation are: β = -0.30, ε = 1.60, ν = 0.00, μ = -0.10, δ = -0.50, and γ_2 = 0.05 [2].

reported in [24]. The spatial profile shown in Figure 7 also contains a transition layer separating two different states [24], which is comparable to the behavior observed in this study. In this system, the defect acts as a pinning mechanism that traps the soliton and helps maintain the front stationary structure instead of forming a symmetric localized pulse.

The front stationary solitons obtained in this study are motivated by the localized solutions reported in earlier works by Akhmediev and Ankiewicz [2], and Renninger [20]. In those studies, stationary solutions were found in systems where stability is supported by higher-order nonlinear effects such as quintic saturation [2][24]. In contrast, the present model considers a cubic system with drift and defect terms, which modifies the behavior of localized profiles without introducing higher-order nonlinearities. These earlier studies provided the motivation for this work, showing that stable stationary fronts can exist under certain parameter ranges [24]. In Renninger's study, stationary solitons were obtained using a hyperbolic cosine ansatz in the cubic-quintic CGLE, while Akhmediev and Ankiewicz [2] studied stationary solitons in the complex Swift-Hohenberg equation (CSHE). These studies provide useful references for understanding localized structures in dissipative systems. Other recent studies [21][22] also observed stationary solitons in dissipative systems, exhibiting behavior comparable to that reported here. The results in Figures 1 – 6 indicate that the obtained solitons remain localized and maintain a front-like structure across different parameter values of B, with variations mainly affecting width and amplitude.

The presence of drift and defect supports the formation of stationary soliton. The balance between gain, loss, nonlinearity, and dispersion together with drift and defect helps maintain a front stationary soliton structure within the considered parameter range. This shows that electromagnetic drift influences the spatial behavior of the soliton profile and is related to the modified area theorem. The ansatz-based formulation used in this study gives a simple approximate solution of the stationary soliton profiles, following Renninger [20]. The soliton profiles remain localized, with small changes in width and amplitude when the parameter B is changed. This shows that the ansatz can describe the main features of stationary localized structures in the CCGLE with drift and defect.

For comparison, Figures 8 and 9 present the stationary soliton solutions reported by Akhmediev and Ankiewicz [2] and Renninger [20], respectively. Their results illustrate stable stationary under their chosen models, providing a reference point for the solitons obtained in the present work. Overall, the approximate ansatz-based solution of this study is consistent with previous studies, while extending the model by including drift and defect effects.

4. CONCLUSIONS

This paper presents the cubic complex Ginzburg-Landau equation (CCGLE) with drift and defect mechanisms. The soliton area theorem is applied to the non-integrable CCGLE, and an approximate ansatz-based approach is used to study the dissipative soliton solutions. From this approach, the soliton energy *E(B)* and soliton duration *T(B)* are derived to characterize their dependence on the shape parameter B. The obtained ansatz-based solutions show the evolution of the soliton profile as B is varied. In addition, the variation of the drift parameter c is investigated to observe the propagation behavior of the front in the system. The results suggest that front stationary solitons can still exist for different values of c. Although the soliton width and peak intensity change, the obtained soliton structures remain localized throughout the propagation. These findings indicate that drift and defect mechanisms do not necessarily need to directly balance each other, but instead interact through a self-organization process to support the formation of front stationary solitons. This behaviour is align with the fundamental concept of dissipative soliton systems with infinite degrees of freedom and provides further understanding of front-like stationary dissipative structures in nonlinear dissipative systems.

AUTHOR INFORMATION

Corresponding Author

Nur Izzati Khairudin — Center of Mathematical Sciences, Universiti Teknologi MARA Perlis Branch, Perlis-02600 (Malaysia);
orcid.org/0000-0001-6619-7094
Email: zatkhairudin@uitm.edu.my

Authors

Nonis Airina Mohd Arshad — Center of Mathematical Sciences, Universiti Teknologi MARA Perlis Branch, Perlis-02600 (Malaysia);
orcid.org/0009-0009-2322-1248
Ahmad Fateh Mohamad Nor — Department of Electrical Engineering, Universiti Tun Hussein Onn Malaysia, Johor-84600 (Malaysia);
orcid.org/0000-0001-8979-4123
Nazirah Ramli — Centre of Mathematical Sciences, Universiti Teknologi MARA Pahang Branch, Pahang-26400 (Malaysia);
orcid.org/0000-0001-8800-7431

Author Contributions

Conceptualization, Methodology, Software, Formal Analysis, Writing – Original Draft Preparation, N. A. M. A.; Validation, Visualization, N. A. M. A. and N. I. K.; Writing – Review & Editing, A. F. M. N., N. R. and N. I. K.; Project

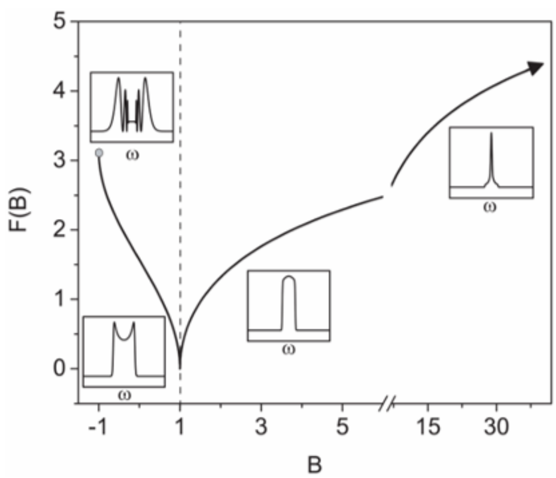

Figure 9. Variation of the pulse energy as a function of the pulse parameter B. Solutions with $|B| < 1$ are separated by a dotted line from those with $B > 1$ [20].

Administration, A. F. M. N.; Supervision, Funding Acquisition, N. I. K.

Conflicts of Interest

The authors declare no conflict of interest.

SUPPORTING INFORMATION

Supplementary data associated with this article can be found in the online version at doi: 10.47352/jmans.2774-3047.463

ACKNOWLEDGEMENT

The authors acknowledge support of the Fundamental Research Grant Scheme for Young Researchers (FRGS-EC) (FRGS EC/1/2024/STG06/UITM/02/15) under the Ministry of Higher Education Malaysia and Universiti Teknologi MARA.

DECLARATION OF GENERATIVE AI

During the preparation of this work, the author used generative AI (ChatGPT by OpenAI) to assist in language refinement and improving the readability of the manuscript. All outputs were reviewed and edited by the author, who takes full responsibility for the content of this publication.

REFERENCES

[1] E. N. Tsoy, A. Ankiewicz, and N. Akhmediev. (2006). "Dynamical Models for Dissipative Localized Waves of the Complex Ginzburg-Landau Equation". *Physical Review E: Statistical, Nonlinear, and Soft Matter Physics.* **73** (3): 036621. 10.1103/PhysRevE.73.036621.

[2] N. Akhmediev and A. Ankiewicz. (2005). In: "Dissipative Solitons, vol. 661". Berlin, Heidelberg: Springer. 1–17. 10.1007/10928028_1.

[3] N. Akhmediev and A. Ankiewicz. (2008). In: "Dissipative Solitons: From Optics to Biology and Medicine, vol. 751". Berlin, Heidelberg: Springer. 1–28. 10.1007/978-3-540-78217-9_1.

[4] N. Akhmediev, A. Ankiewicz, and J. M. Soto-Crespo. (1997). "Multisoliton Solutions of the Complex Ginzburg-Landau Equation". *Physical Review Letters.* **79** (21): 4047–4051. 10.1103/PhysRevLett.79.4047.

[5] N. Akhmediev, A. Ankiewicz, J. M. Soto-Crespo, and P. Grelu. (2009). "Dissipative Solitons: Present Understanding, Applications and New Developments". *International Journal of Bifurcation and Chaos.* **19** (8): 2621–2636. 10.1142/S0218127409024372.

[6] I. S. Aranson and L. Kramer. (2002). "The World of the Complex Ginzburg-Landau Equation". *Reviews of Modern Physics.* **74** (1): 99–143. 10.1103/RevModPhys.74.99.

[7] M. Facao and M. I. Carvalho. (2017). "Plain and Oscillatory Solitons of the Cubic Complex Ginzburg-Landau Equation with Nonlinear Gradient Terms". *Physical Review E.* **96** (4): 042220. 10.1103/PhysRevE.96.042220.

[8] V. Skarka, N. B. Aleksić, H. Leblond, B. A. Malomed, and D. Mihalache. (2010). "Varieties of Stable Vortical Solitons in Ginzburg-Landau Media with Radially Inhomogeneous Losses". *Physical Review Letters.* **105** (21): 213901. 10.1103/PhysRevLett.105.213901.

[9] H. Rezazadeh. (2018). "New Solitons Solutions of the Complex Ginzburg-Landau Equation with Kerr Law Nonlinearity". *Optik: International Journal for Light and Electron Optics.* **167** : 218–227. 10.1016/j.ijleo.2018.04.026.

[10] D. Zanga, S. I. Fewo, C. B. Tabi, and T. C. Kofané. (2022). "Generation of Dissipative Solitons in a Doped Optical Fiber Modelled by the Higher-Order Dispersive Cubic-Quintic-Septic Complex Ginzburg-Landau Equation". *Physical Review A.* **105** (2): 023502. 10.1103/PhysRevA.105.023502.

[11] E. M. E. Zayed, K. A. Gepreel, M. El-Horbaty, and M. E. M. Alngar. (2023). "Highly Dispersive Optical Solitons in Birefringent Fibers of Complex Ginzburg-Landau Equation of Sixth Order with Kerr Law Nonlinear Refractive Index". *Eng.* **4** (1): 665–677. 10.3390/eng4010040.

[12] I. M. Uzunov and S. G. Nikolov. (2020). "Influence of the Higher-Order Effects on the Solutions of the Complex Cubic-Quintic Ginzburg-Landau Equation". *Journal of Modern Optics.* **67** (7): 606–618. 10.1080/09500340.2020.1760385.

[13] P. Parra-Rivas, D. Gomila, L. Gelens, M. A. Matías, and P. Colet. (2015). In: "Nonlinear Optical Cavity Dynamics: From Microresonators to Fiber Lasers". Wiley. 107 –128. 10.1002/9783527686476.ch5.

[14] P. Parra-Rivas. (2017). "Dynamics of Dissipative Localized Structures in Driven Nonlinear Optical Cavities". VUB Press.

[15] P. Parra-Rivas, D. Gomila, M. A. Matías, and P. Colet. (2013). "Dissipative Soliton Excitability Induced by Spatial Inhomogeneities and Drift". *Physical Review Letters.* **110** (6): 064103. 10.1103/PhysRevLett.110.064103.

[16] P. Parra-Rivas, D. Gomila, M. A. Matías, P. Colet, and L. Gelens. (2014). "Effects of Inhomogeneities and Drift on the Dynamics of Temporal Solitons in Fiber Cavities and Microresonators". *Optics Express.* **22** (25): 30943–30954. 10.1364/OE.22.030943.

[17] P. Parra-Rivas, D. Gomila, M. A. Matías, P. Colet, and L. Gelens. (2016). "Competition Between Drift and Spatial Defects Leads to Oscillatory and Excitable Dynamics of Dissipative Solitons". *Physical Review E.* **93** (1): 012211. 10.1103/PhysRevE.93.012211.

[18] G. P. Agrawal. (2001). In: "Nonlinear Fiber Optics, 3 ed.". Academic Press. 31–62. 10.1016/B978-012045144-9/50002-3.

[19] M. I. Carvalho, M. Facão, and O. Descalzi. (2025). "Dissipative Solitons Onset Through Modulational Instability of the Cubic Complex Ginzburg-Landau Equation with Nonlinear Gradients". *Chaos: An Interdisciplinary Journal of Nonlinear Science.* **35** (9). 10.1063/5.0278588.

[20] W. H. Renninger, A. Chong, and F. W. Wise. (2010). "Area Theorem and Energy Quantization for Dissipative Optical Solitons". *Journal of the Optical Society of America B: Optical Physics.* **27** (10): 1978–1982. 10.1364/JOSAB.27.001978.

[21] N. A. Kudryashov. (2022). "Exact Solutions of the Complex Ginzburg-Landau Equation with Law of Four Powers of Nonlinearity". *Optik: International Journal for Light and Electron Optics.* **265** : 169548. 10.1016/j.ijleo.2022.169548.

[22] Y. Wang, Z. Yin, L. Lu, and Y. Kai. (2024). "Dynamic Properties and Chaotic Behaviors of Pure-Cubic Complex Ginzburg-Landau Equation with Different Nonlinearities". *Results in Physics.* **64** : 107913. 10.1016/j.rinp.2024.107913.

[23] A. Pakhomov, M. Arkhipov, N. Rosanov, and R. Arkhipov. (2023). "Area Theorem in a Ring Cavity". *Physical Review A.* **108** : 023506. 10.1103/PhysRevA.108.023506.

[24] W. Van Saarloos and P. C. Hohenberg. (1992). "Fronts, Pulses, Sources, and Sinks in Generalized Complex Ginzburg-Landau Equations". *Physica D: Nonlinear Phenomena.* **56** (4): 303–367. 10.1016/0167-2789(92)90175-M.

[25] E. Yomba and G. A. Zakeri. (2013). "Exact Solutions in Nonlinearly Coupled Cubic-Quintic Complex Ginzburg-Landau Equations". *Physics Letters A.* **377** (3-4): 148 –157. 10.1016/j.physleta.2012.11.041.